

ORGANIC GEOCHEMISTRY AND DEPOSITIONAL ARCHITECTURE OF JIMUSAER OIL SHALE, JUNGGAR BASIN, NW CHINA

WEI KONG^(a,b), DANFENG TU^(c), YANGLU WAN^{(d)*},
YUNBIN ZHAO^(b), XIAOLIN ZANG^(b)

- ^(a) Chengdu University of Technology, College of Energy Resources, Chengdu 610059, China
^(b) CNOOC Ener Tech-Drilling & Production Co., Tianjin 300452, China
^(c) Bohai Oilfield Research Institute, Tianjin Branch Company, CNOOC China Ltd, Tianjin City, 300452, China
^(d) Wuxi Institute of Petroleum Geology, SINOPEC, Wuxi 214126, China

Abstract. *The Jimusaer oil shale (JOS) of the Upper Permian Lucaogou Formation in the southeastern margin of the Junggar Basin, Northwest China has retained a close relationship with the Bogda orogeny. JOS samples were studied for organic geochemistry, and samples of other rocks collected from between the oil shale layers (sandstone, mudstone shale, dolostone, limestone) were investigated for mineral characteristics. The results showed JOS samples to have a high total organic carbon (TOC) content, 5.35–21.45%, and a high oil yield, 3.67–10.3%. Dolomite, clay minerals, quartz, tuffaceous matrix, tuff debris, calcite, ferruginous debris, siliceous debris and anorthose could be found in the samples of other rocks. The Jimusaer oil shale was characterized by fine grain size, dark color and horizontal bedding. Depositional architecture and symbiotic rocks indicated that JOS was mainly deposited in a semi-deep to deep water environment under reducing conditions. The oil shale developed in the highstand systems tract (HST) and was enriched in organic matter.*

Keywords: *Jimusaer oil shale, geochemical characteristics, mineralization, stratigraphic sequence, depositional architecture.*

1. Introduction

With its oil shale resources, China ranks fourth in the world. The Junggar Basin is one of the largest oil shale basins in China and has great development prospects [1, 2]. The oil shale deposit is located in the area of 143 km (length) × 10 to 20 km (width), contains 548×10^8 t of shale oil

* Corresponding author: e-mail wanyl.syky@sinopec.com, 995913661@qq.com

resource at the northern foot of Bogda Mountain in the southern Junggar Basin and includes, from west to east, Yaomoshan, Shuimogou, Lucaogou, Dongshan, Dadonggou, Sangonghe, Sigonghe, Wugonghe, Dahuangshan, and Jimusaer mining areas (Fig. 1a) [3–6]. Oil shale occurs in the Upper Permian Lucaogou Formation (P_2l) whose lithology is mainly made up of gray-black oil shale, dolostone, dolomitic sandstone, dolomitic siltstone, sporadic pyrite, tuff, and shale argillaceous siltstone containing bitumen. The total thickness of oil shale in the Lucaogou Formation in the Jimusaer mining area is greater than that in Dahuangshan [7]. According to lithologic characteristics, the sequences of the Jimusaer Lucaogou Formation can be divided into six segments from bottom to top whereas only four segments can be found in the Fukang mining area (Fig. 1a), which mainly resulted from the migration of subsidence and depocenter (Fig. 2).

The Jimusaer oil shale (JOS) in the southern margin of the Junggar Basin is deposited in the front of the thrust nappe structure in the orogenic belt of the Meso-Cenozoic North Tianshan Bogda Mountain [2]. JOS has retained a close relationship with the Bogda orogeny (Fig. 3). The evolution of the basin and the spatial distribution of the sediments have been determined by the paleotectonic background. The paleotectonic background has also influenced the distribution and geometry of the basin depression and has determined the types of organic matter in oil shale [8]. Since the Late Palaeozoic the southern margin of the Junggar Basin has undergone multi-stage tectonic processes related to the orogenies in the Hercynian, Indosinian, Yanshanian and Himalayan. During those periods, the extensional, compressional and shearing forces led to the formation of complex structures in the Jimusaer mining area. From the Carboniferous to the Early Permian age, the Bogda rift transformed into a residual sea in this area. During the deposition of Lucaogou and Hongyanchi formations, the Jimusaer area provided a stable lacustrine environment with deep fresh brackish water, which was beneficial for the proliferation and preservation of organic matter. During the Late Permian, in front of Bogda Mountain, the stable lacustrine environment and tectonic system of the thrust nappe structure favored the deposition and preservation of oil shale. In the Late Cretaceous, Bogda Mountain became active and its piedmont region entered the tectonic phase. The Himalayan orogeny led to the appearance of multiple rows of the thrust fold zone in the piedmont region, the intense uplift of the foreland basin, and the exposure of oil shale [2].

However, the organic geochemistry and depositional architecture of JOS in the northern Bogda Mountain have rarely been paid attention to. The Jimusaer oil shale mining area from west to east, including Shichanggou and Wujiawan zones, has been chosen as the main target of this paper (Fig. 1b). More specifically, the study focuses on the sedimentary environment and lithology of the area, the parameters of hydrocarbon source rock and the characteristics of minerals, as well as aims at revealing the enrichment mechanisms in JOS and establishing its enrichment model.

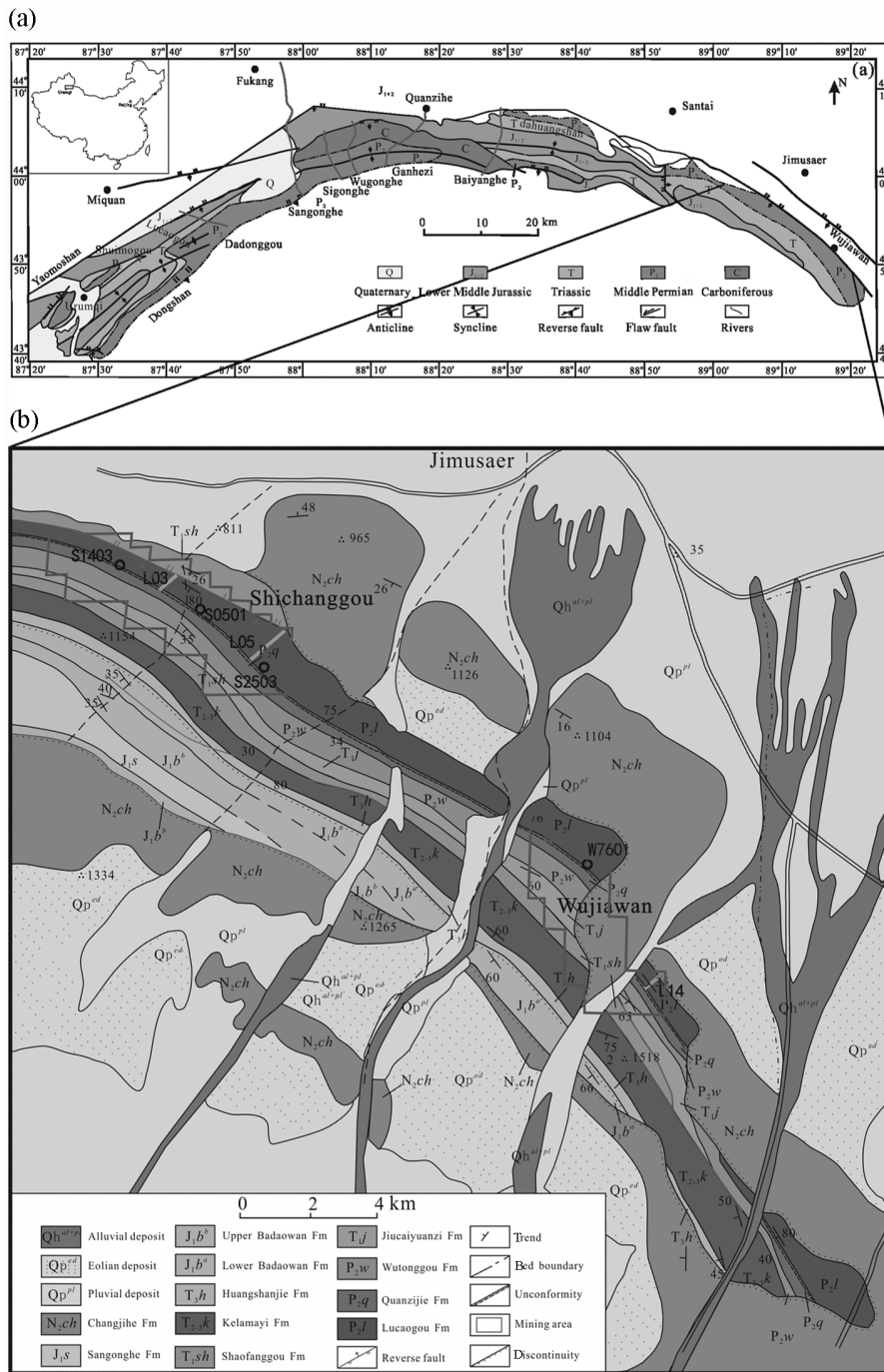


Fig. 1. (a) Generalized map of oil shale mining areas in the southern Junggar Basin; (b) simplified geological map of the Jimusaer area, showing the location of Shichanggou and Wujiawan oil shale mining areas. (The abbreviation used: Fm – Formation.)

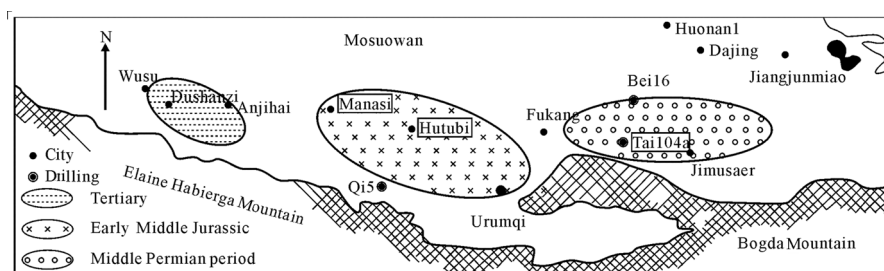


Fig. 2. Changes of subsidence centres and depocentre from the Permian to the Tertiary in the southern Junggar Basin (modified from [3]).

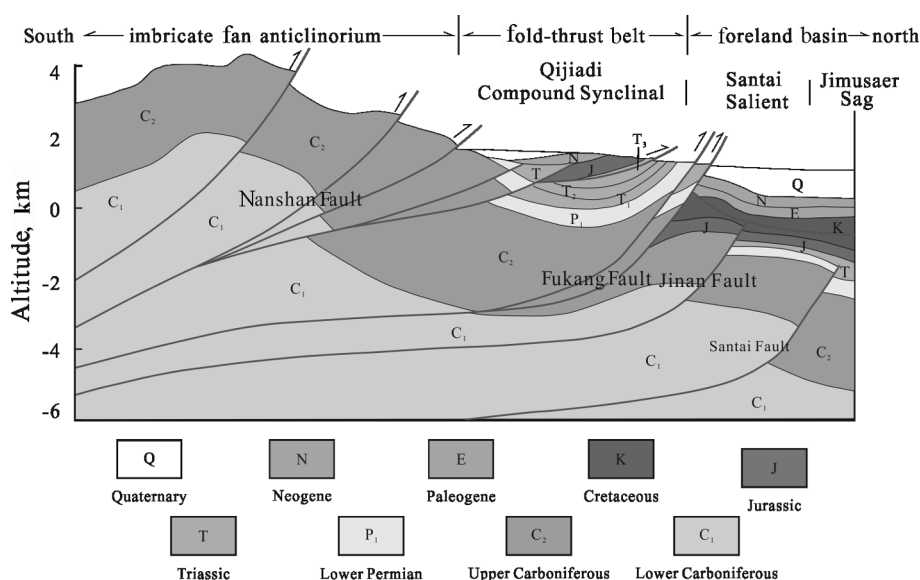


Fig. 3. The general geological profile of the Bogda Mountain foot in the Jimusaer area.

2. Samples and tests

The distribution of the Jimusaer oil shale mining area is shown in Figure 1b. For the study, 60 oil shale samples and 30 samples of other rocks (sandstone, mudstone shale, dolostone, limestone) were collected from four drillings: S0501, S1403, S2503 and W7601 (Fig. 1b). All the samples were stored in plastic bags to ensure as little contamination and oxidation as possible. All the oil shale samples were crushed into particles smaller than 200 mesh for Gray-King low-temperature distillation, total organic carbon (TOC) determination and Rock-Eval pyrolysis. 26 samples from all oil shale layers were collected from drillings S1403 and W7601. According to Chinese National standard methods GB/T 19145-2003 and GB/T 18602-2001, the TOC determination and Rock-Eval pyrolysis were performed on a Rock-Eval II instrument following the procedure set in [9]. The mineral composition of

30 samples of other rocks collected from between the oil shale layers was determined by optical microscopic observation using polarized light.

3. Results and discussion

3.1. Rock-Eval pyrolysis, TOC and oil yield

The values of parameters S_1 , S_2 , S_3 , hydrogen index (HI), oxygen index (OI), production index (PI) and T_{max} were obtained through Rock-Eval pyrolysis [10]. Rock-Eval data, TOC and oil yield of 26 samples are presented in the Table. The analysis of the samples showed that oil shale had a relatively

Table. Oil yield, TOC and Rock-Eval data about 26 Jimusaer oil shale samples

Sample No.	Oil yield, %	TOC, wt%	S_1 , mg HC/g rock	S_2 , mg HC/g rock	S_3 , mg CO ₂ /g rock	HI, mg HC/g TOC	OI, mg CO ₂ /g TOC	PI, $S_1/(S_1 + S_2)$	T_{max} , °C
OW-01	5.75	8.42	0.47	34.3	2.51	407.36	29.81	0.014	441
OW-02	5.62	7.94	0.68	49.32	1.89	621.16	23.80	0.014	436
OW-03	7.56	11.01	0.43	78.32	1.52	711.04	13.80	0.005	437
OW-04	8.43	12.28	0.79	90.46	2.69	736.49	21.90	0.009	437
OW-05	9.39	13.68	0.26	84.25	1.05	615.81	7.67	0.003	429
OW-06	5.82	8.48	0.61	29.44	1.21	347.18	14.27	0.020	438
OW-07	6.01	8.76	0.16	59.45	0.99	678.92	11.31	0.003	429
OW-08	5.14	7.49	0.76	37.47	1.58	500.34	21.10	0.020	435
OW-09	4.66	6.79	1.27	31.21	3.04	459.67	44.77	0.039	431
OW-10	10.01	21.45	0.28	95.93	2.96	447.23	13.80	0.003	436
OW-11	9.5	16.94	0.39	128.87	1.95	760.68	11.51	0.003	433
OW-12	7.53	10.97	0.61	76.98	0.96	701.65	8.75	0.008	435
OW-13	4.72	6.88	0.96	22.71	4.32	330.23	62.82	0.041	433
OW-14	9.15	19.78	0.67	108.63	3.26	549.19	16.48	0.006	429
OW-15	9.48	13.81	1.04	99.46	4.05	720.08	29.32	0.010	432
OS-01	7.07	10.30	0.69	51.53	4.56	500.24	44.27	0.013	428
OS-02	9.35	13.62	0.52	75.87	3.65	556.93	26.79	0.007	436
OS-03	5.55	8.09	0.73	54.96	2.95	679.66	36.48	0.013	433
OS-04	3.67	5.35	0.26	59.13	5.16	1105.81	96.50	0.004	442
OS-05	5.83	8.49	0.95	80.56	2.1	948.40	24.72	0.012	435
OS-06	6.77	9.86	0.52	71.17	2.97	721.52	30.11	0.007	436
OS-07	10.3	15.01	0.98	106.75	3.56	711.33	23.72	0.009	428
OS-08	7.59	11.06	0.35	97.17	4.89	878.68	44.22	0.004	432
OS-09	5.86	8.54	0.19	93.68	1.69	1097.21	19.79	0.002	436
OS-10	6.33	9.22	0.3	76.64	2.53	830.98	27.43	0.004	429
OS-11	5.88	8.57	0.44	64.06	2.84	747.74	33.15	0.007	432

Note: S_1 = free hydrocarbons; S_2 = pyrolysis hydrocarbon; S_3 = carbon dioxide; TOC = total organic carbon; T_{max} = temperature of maximum S_2 ; PI = productivity index ($PI = S_1/(S_1 + S_2)$); HI = hydrogen index ($HI = [S_2/TOC] \times 100$); OI = oxygen index ($OI = [S_3/TOC] \times 100$).

high oil yield, 3.67–10.30%. The mean oil yield (7.04%) of this oil shale was higher than that of marine oil shale (6.80%) from the Changshe Mountain mining area in the northern Qiangtang Depression of the Tibet Plateau [11, 12]. TOC varying from 5.35 to 21.45 wt% (mean 10.88 wt%) was calculated by the sum of pyrolytic and residual organic carbons. Rock-Eval S_1 and S_2 were respectively 0.16–1.27 and 22.71–128.87 mg HC/g rock. HI ranged widely, from 330.23 to 1105.81 mg HC/g TOC. The values of TOC, S_2 , HI and oil yield of the samples showed JOS to have a significant resource potential. The extremely low PI values (0.002–0.041) (Table) showed that the oil shale organic material in the studied mining area was immature whereas the high T_{max} values (428–442 °C) (Table) implied that oil shale was in the early- to medium-maturity stage [13, 14].

The determination of kerogen types was entirely based on HI. The graph of S_2 vs TOC was used to show the types and hydrocarbon potential of kerogen (Fig. 4) [15]. As seen from Figure 4, the kerogen types of the samples were between I and II, suggesting that the Jimusaer source rock had a high oil-prone potential. The HI vs T_{max} plot was used to reflect the quality and maturity of kerogen (Fig. 5). As Figure 5 reveals, the samples were in the immature to low-maturity stage, which is equivalent to the vitrinite reflectance (R_o) of about 0.65% R_o [16].

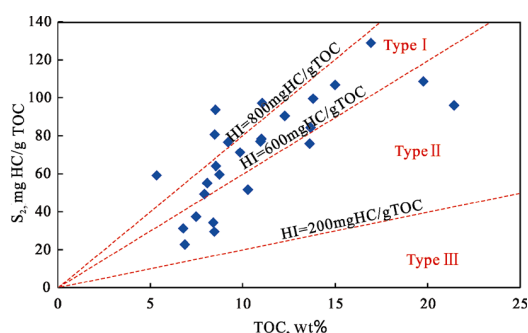


Fig. 4. Plot of S_2 vs TOC indicating the kerogen types of Jimusaer oil shale.

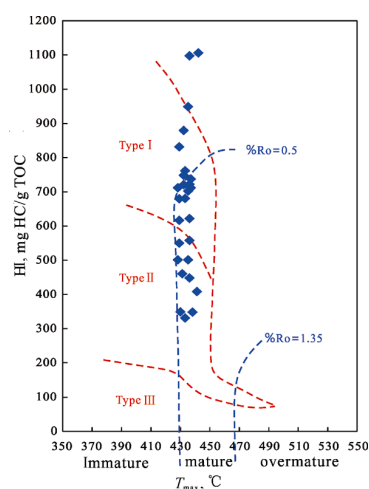


Fig. 5. Plot of HI vs T_{max} indicating the kerogen types and maturity of Jimusaer oil shale.

3.2. Mineral characteristics of the Lucaogou Formation

The Lucaogou Formation consists of sandstone, mudstone shale, oil shale, dolostone, limestone and tuff. Tuffaceous debris and tuffite are widely distributed in sandstone, mudstone and carbonatite lithologies. Organic matter including mineral nutrients and aquatic organisms can increase biopro-

ductivity, while terrigenous and aquatic organic matters determine kerogen types [17]. The analysis of JOS samples showed that with increasing HI the kerogen type changed, but the corresponding correlation between TOC and HI did not exist (Fig. 6). This indicated that organic matter in JOS was enriched and the samples were less influenced by its original nature. Therefore, volcanoes must have had an influence on the oil shale formation and the input of volcanic ash probably provided a sufficient amount of nutrients for the growth of algae.

The sandstone lithology in the studied area included argillaceous siltstone, dolomitic lithic sandstone and dolomitic siltstone. Argillaceous siltstone had a high content of terrigenous detrital minerals and the interstitial materials were mainly made up of clay minerals and some amount of authigenic quartz. In addition, volcanic debris, siliceous fragments, quartz particles and feldspars were widely distributed in dolomitic lithic sandstone. Dolomitic siltstone consisted of terrigenous debris and was chiefly cemented by dolomite. Mudstone and shale, which also contained quartz and silty, calcareous and dolomitic materials, had a high content of clay minerals. Calcite, hypocrySTALLINE dolomite particles and tuffaceous materials were abundant in mudstone. Dispersed volcanic ash and tuffaceous debris could be found in tuffaceous mudstone (Fig. 7a–b). In the Jimusaer mining area, three types of dolostone were found: micritic dolostone, sandy aplitic dolostone and tuffaceous dolostone. The appearance of quartz, plagioclase and tuffaceous and siliceous fragments in the area showed that dolomite containing some ferruginous debris (Fig. 7c–d) had apparent sedimentary characteristics. In the mining area, two kinds of limestone could be distinguished: micritic limestone and fine breccia limestone. Quartz and ferruginous organic debris were found in micritic limestone whose cement was a mixture of cryptocrystalline calcite and clay minerals. The fine breccia limestone was mostly composed of calcite oolites with tuff debris

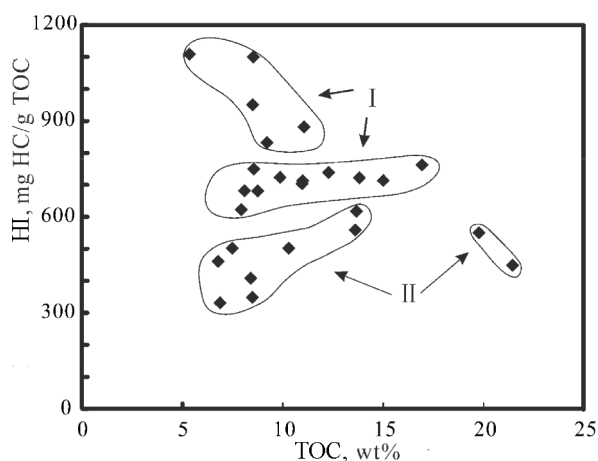


Fig. 6. Plot of TOC vs HI of Jimusaer oil shale.

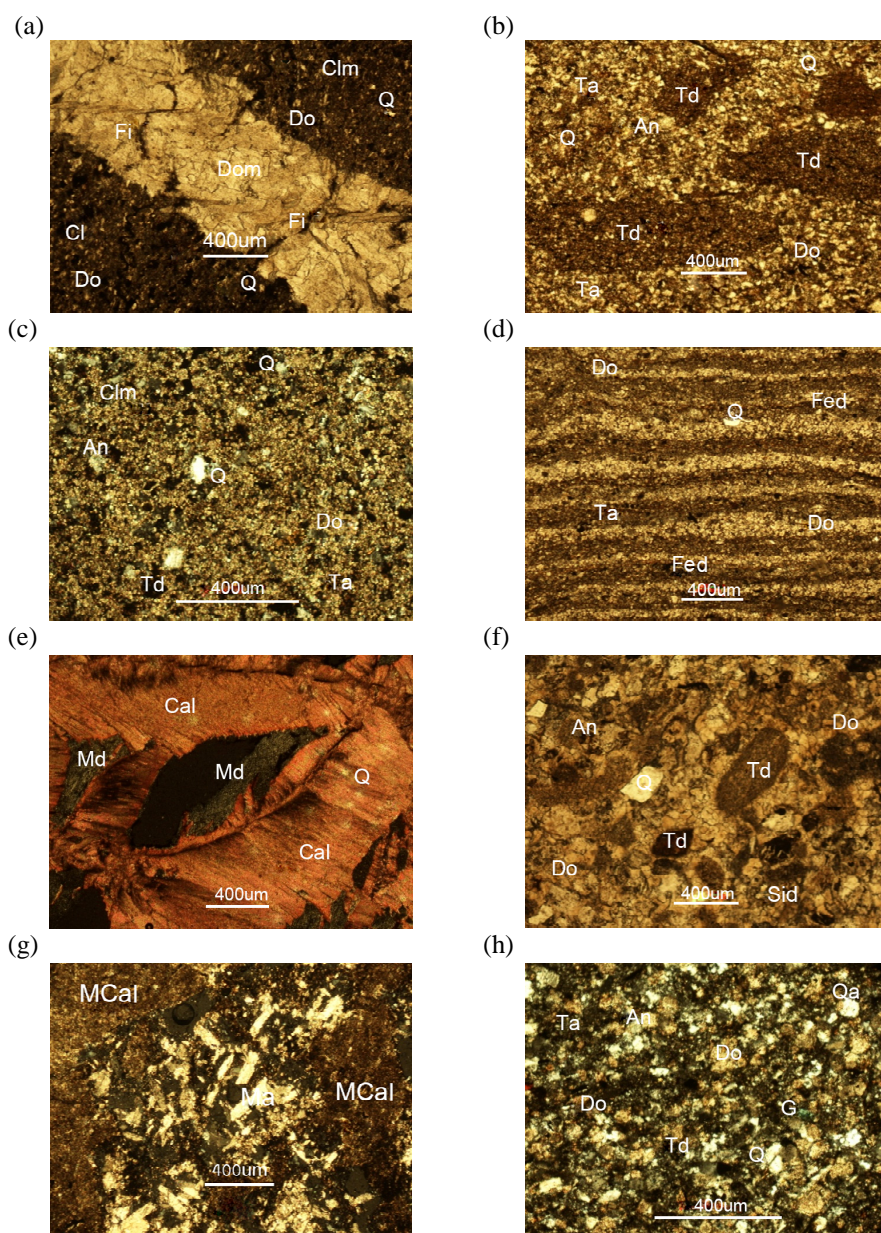


Fig. 7. Major minerals and rocks of the Lucaogou Formation in the Jimusaer oil shale mining area: (a) dolomitic mudstone with dolomite veins (Dom), clay minerals (CIm), quartz (Q), dolomitic (Do) and fissures development (Fi); (b) tuffaceous mudstone with tuff debris (Td), quartz, dolomitic and tuffaceous matrix (Ta); (c) sandy aplitic dolostone with quartz, dolomitic, tuff debris, tuffaceous matrix and anorthose (An); (d) tuffaceous dolostone with dolomitic, tuffaceous matrix, quartz and ferruginous debris (Fed); (e) breccia limestone veins with fibrous calcite (Cal), quartz and mudstone debris (Md); (f) fine breccia dolostone with quartz, anorthose, tuff debris, siliceous debris (Si) and dolomitic; (g) micritic limestone with micritic calcite (MCal), clay minerals and magnesite (Ma); (h) dolomitic tuffite with quartz, anorthose, tuff debris, tuffaceous matrix, authigenic quartz (Qa) and glauconite (G).

(Fig. 7e–g). The two kinds of volcanic tuff – dolomitic tuffite and silty tuffite – contained quartz, plagioclase and ferruginous debris. Tuff debris was the main component of volcanic tuff, and the tuffaceous matrix was the cement of the skeleton touch space (Fig. 7h).

3.3. Sedimentary environment of the Lucaogou Formation

In the Permian, the Jimusaer Lucaogou Formation sequence was divided into six sections from bottom to top according to lithologic characteristics: dolostone (P_2l^1), dolostone interbedded with sandstone (P_2l^2), lower oil shale (P_2l^3), sandstone (P_2l^4), upper oil shale (P_2l^5) and shale (P_2l^6) (Fig. 8). P_2l^3 and P_2l^5 contained the main workable oil shale segments. Generally, the thickness of oil shale in P_2l^3 was greater than that in P_2l^5 , while from west to east the oil shale thickness in the latter became too thin to develop the rock economically. P_2l^4 consisted of a series of sandstone layers. In the Early Late

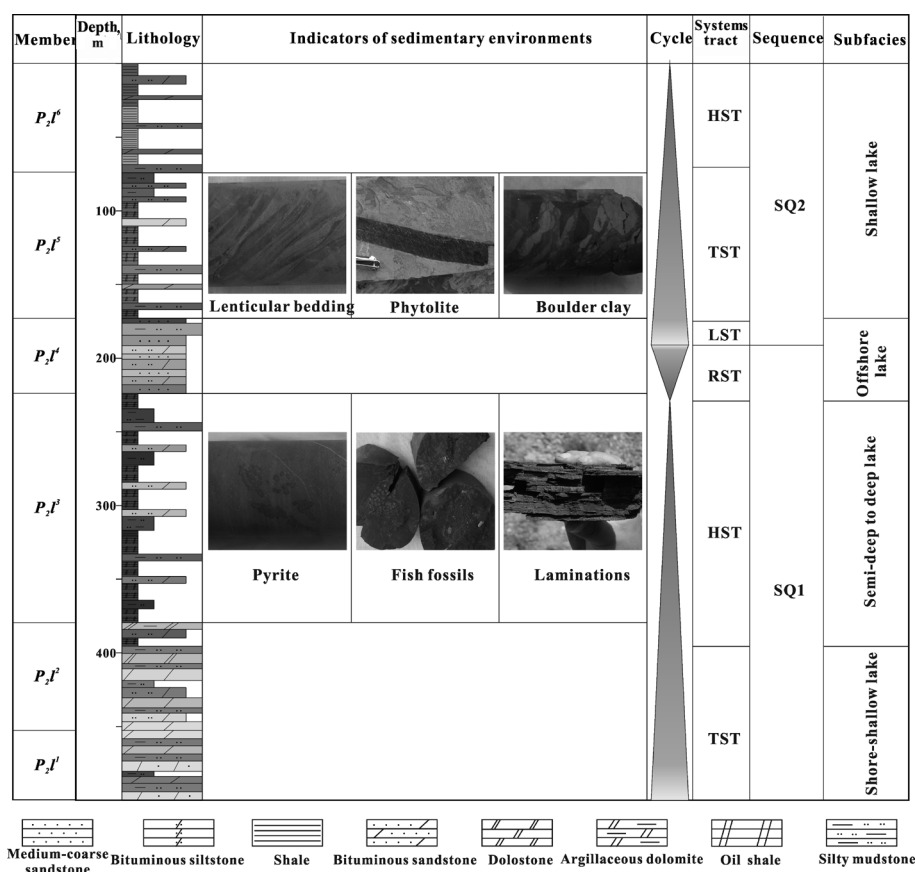


Fig. 8. Sequence of the Lucaogou Formation in the Jimusaer oil shale mining area. (The abbreviations used: HST – highstand systems tract, TST – transgressive systems tract, LST – lowstand systems tract, RST – regressive systems tract.)

Permian, the input of tephra had provided abundant nutrients for the vigorous growth of plants and also provided algae for adequate organic matter. The Jimusaer oil shale is generally characterized by fine grain size, dark color, organic richness, and horizontal bedding (Fig. 9a). The fact that lamellibranchiate fossil (Fig. 9b), fish skeletal fossil (Fig. 9c) and siderite (Fig. 9d) are abundant in argillaceous rock suggests that the oil shale should have been deposited in fresh brackish water and an anaerobic environment under propitious hydrodynamic conditions. HI may reflect the types of redox conditions [17], and generally, a high HI (avg 667.9 mg HC/g TOC) (Table) may point to a reducing environment during the deposition of P₂l. Additionally, based on the contents of major and trace elements, some researchers have suggested that JOS was deposited in an anoxic lacustrine environment in a warm humid climate [2].

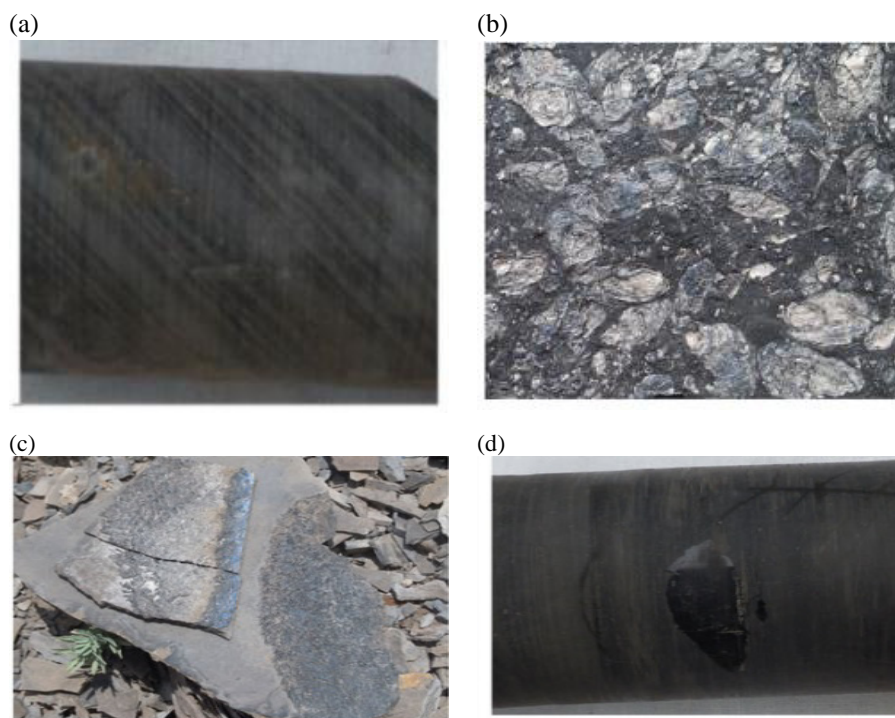


Fig. 9. Features of Jimusaer argillaceous rock from semi-deep to deep lake facies: (a) horizontal bedding, (b) lamellibranchiate fossils, (c) dish skeletal fossils, (d) siderite concretion.

3.4. Depositional architecture model of Jimusaer oil shale

The research on depositional framework can be used to predict the geometry and continuity of oil shale deposition, as well as its resource potential. The formation of oil shale was controlled by the accumulation and preservation

of organic matter and required a delicately balanced subsidence rate at an optimum water table level. A comprehensive method for characterizing the sediments, tectonic structures and symbiotic rocks was employed to establish the depositional architecture model of JOS.

The outcrops of the Lucaogou Formation in the Jimusaer oil shale mining area (L03, L05 and L14 in Fig. 1b) provided conditions for the research of sequence (SQ) stratigraphy. The markers of sequence stratigraphy collected from the outcrops were applied to build the sequence stratigraphic framework. Therefore, both two third-order sequences and six systems tracts corresponding to different depositional facies were identified. The change of the depositional environment can be inferred from the changes in sedimentary lithology. Thus, the sequence boundary between SQI and SQII could be identified in the upper part of P_2l^4 (Fig. 8). Above the boundary, coarse-grained sandstone composed of feldspars and quartz was identified as the incised valley filling in the lowstand systems tract (LST), while under the boundary, bituminous siltstone interbedded with silty mudstone was deposited in a lakeshore environment. Obviously, there must have been a discontinuity between SQI and SQII. The sediments were deposited in the accommodation space controlled by the base level. The sediments of the prograding sequence coarsened, leading to the formation of the oil shale layer of low economic value. The transgressive systems tract (TST) and the highstand systems tract (HST) contained abundant fossils. TST in its late stage and HST included a condensed section containing some amount of coarse terrigenous clastic sediments, and were enriched in organic matter; so, oil shale was developed in TST and HST (Fig. 8). In the progradational sequence, the sedimentary particles generally coarsened and oil shale segments were rarely developed in the regressive systems tract (RST) and LST.

The activities of the thrust nappe tectonic belt in front of Bogda Mountain led to basement subsidence and large transgression. During the deposition of P_2l^3 , the basin was in a warm humid climate and a stable ecological environment, providing steady deep water conditions with relatively abundant aquatic organisms [2]. Thus, oil shale with horizontal bedding, a stable distribution and a great sedimentary thickness was rich in organic matter (Fig. 9). Climate and water level changes resulted in the deterioration of the quality of oil shale in P_2l^5 and its discontinuous distribution in the Jimusaer area. JOS was mainly developed in a semi-deep to deep water environment, while deposited in a shallow to semi-deep water environment, its quality was slightly poorer, in terms of thickness, oil yield and TOC. From the mineral features of the Lucaogou Formation it can be inferred that a volcano should have had an influence on the accumulation and preservation of oil shale (Fig. 10).

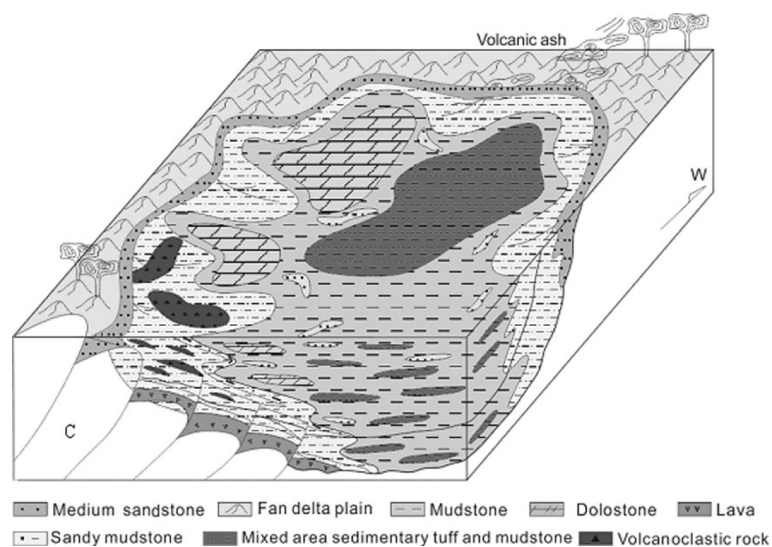


Fig. 10. Depositional architecture model of oil shale in the Jimusaer mining area.

4. Conclusions

In this study, the mean values of oil yield, total organic carbon and $S_1 + S_2$ of Jimusaer oil shale were found to be respectively 7.04%, 10.88 wt% and 72.06 mg HC/g rock, its kerogen types were mainly I and II, and T_{max} value was around 435 °C. All these parameter values indicated Jimusaer oil shale to be rich in low-maturity organic matter. The uplift of Bogda Mountain provided not only a rich organic matter provenance but also favorable terrain conditions for accumulation and preservation of oil shale. The lithology of the Lucaogou Formation consisted of sandstone, mudstone shale, oil shale, dolostone, limestone and tuff. These rocks contained dolomite, clay minerals, quartz, tuffaceous matrix, tuff debris, calcite, ferruginous debris, siliceous debris and anorthose. The key sequence stratigraphy boundaries were identified and oil shale was mainly deposited in transgressive and highstand systems tracts. The depositional architecture model of Jimusaer oil shale was established.

REFERENCES

1. Liu, Z. J., Liu, R. Oil shale resource state and evaluating system. *Earth Science Frontiers (China University of Geosciences (Beijing); Peking University)*, 2005, **12**(3), 315–323 (in Chinese, summary in English).
2. Liang, J. L., Tang, D. Z., Xu, H., Tao, S., Li, C. C., Gou, M. F. Formation conditions of Jimusaer oil shale at the northern foot of Bogda Mountain, China. *Oil Shale*, 2014, **31**(1), 19–29.

3. Bai, Y. L. Prospects for development of oil shale deposits in the southeastern margin of Junggar Basin. *Xinjiang Petroleum Geology*, 2008, **29**(4), 462–465 (in Chinese with English abstract).
4. Tao, S., Tang, D. Z., Xu, H., Cai, J. L., Gou, M. F., Chen, Z. L. Retorting properties of oil shale found at the northern foot of Bogda Mountain, China. *Oil Shale*, 2011, **28**(1), 19–28.
5. Tao, S., Wang, Y. B., Tang, D. Z., Xu, H., Zhang, B., He, W., Liu, C. Composition of the organic constituents of Dahuangshan oil shale at the northern foot of Bogda Mountain, China. *Oil Shale*, 2012, **29**(2), 115–127.
6. Wei, X. C., Liu, S. C., Xia, M. The genesis analysis of oil shale in southern Jimisar, Xinjiang. *Xinjiang Geology*, 2012, **30**, 66–70 (in Chinese).
7. Bai, B. *Tectono-Sedimentary Evolution and its Controls on Basic Petroleum Geological Condition of South Margin of Junggar*. PhD Thesis, Northwestern University, 2008 (in Chinese).
8. Scott, A. R. Hydrogeologic factors affecting gas content distribution in coal beds. *Int. J. Coal Geol.*, 2002, **50**(1–4), 363–387.
9. Espitalié, J., Deroo, G., Marquis, F. Rock-Eval pyrolysis and its applications, Part II. *Rev. I. Fr. Pétrol.*, 1985, **40**, 755–784 (in French).
10. Alaug, A. S. Source rocks evaluation, hydrocarbon generation and palynofacies study of late Cretaceous succession at 16/G-1 offshore well in Qamar Basin, eastern Yemen. *Arabian Journal of Geosciences*, 2011, **4**(3–4), 551–566.
11. Fu, X. G., Wang, J., Zeng, Y. H., Tan, F. W., Feng, X. L. REE geochemistry of marine oil shale from the Changshe Mountain area, northern Tibet, China. *Int. J. Coal Geol.*, 2010, **81**(3), 191–199.
12. Tao, S., Tang, D. Z., Xu, H., Liang, J. L., Shi, X. F. Organic geochemistry and elements distribution in Dahuangshan oil shale, southern Junggar Basin: Origin of organic matter and depositional environment. *Int. J. Coal Geol.*, 2013, **115**(8), 41–51.
13. Rippen, D., Littke, R., Bruns, B., Mahlstedt, N. Organic geochemistry and petrography of Lower Cretaceous Wealden black shales of the Lower Saxony Basin: The transition from lacustrine oil shales to gas shales. *Org. Geochem.*, 2013, **63**, 18–36.
14. Bordenave, M. L. *Applied Petroleum Geochemistry*. Editions Technip, Paris, 1993, p 425.
15. Dembicki Jr., H. Three common source rock evaluation errors made by geologists during prospect or play appraisals. *AAPG Bull.*, 2009, **93**(3), 341–356.
16. Bechtel, A., Jia, J., Strobl, S. A. I., Sachsenhofer, R. F., Liu, Z., Gratzner, R., Püttmann, W. Palaeoenvironmental conditions during deposition of the Upper Cretaceous oil shale sequences in the Songliao Basin (NE China): Implications from geochemical analysis. *Org. Geochem.*, 2012, **46**, 76–95.
17. Song, Y., Liu, Z., Meng, Q., Xu, J., Sun, P., Cheng, L., Zheng, G. Multiple controlling factors of the enrichment of organic matter in the Upper Cretaceous oil shale sequences of the Songliao Basin, NE China: implications from geochemical analyses. *Oil Shale*, 2016, **33**(2), 142–166.

Presented by X. Han

Received November 17, 2017